J. Membrane Biol. 195, 121–136 (2003)
10.1007/s00232-003-0614-2

The Journal of
Membrane
Biology

Cu^{2+}, Co^{2+}, and Mn^{2+} Modify the Gating Kinetics of High-Voltage-Activated Ca^{2+} Channels in Rat Palaeocortical Neurons

L. Castelli, F. Tanzi, V. Taglietti, J. Magistretti
Dipartimento di Scienze Fisiologiche-Farmacologiche Cellulari-Molecolari, Sezione di Fisiologia Generale e Biofisica Cellulare, Università degli Studi di Pavia, Via Forlanini 6, 27100 Pavia, Italy

Received: 31 January 2003/Revised: 8 July 2003

Abstract. The effects of three divalent metal cations (Mn^{2+}, Co^{2+}, and Cu^{2+}) on high-voltage-activated (HVA) Ca^{2+} currents were studied in acutely dissociated pyramidal neurons of rat piriform cortex using the patch-clamp technique. Cu^{2+}, Mn^{2+}, and Co^{2+} blocked HVA currents conducted by Ba^{2+} (I_{Ba}) with IC_{50} of ~920 nM, ~58 μM, and ~65 μM, respectively. Additionally, after application of non-saturating concentrations of the three cations, residual currents activated with substantially slower kinetics than control I_{Ba}. As a consequence, the current fraction abolished by the blocking cations typically displayed, in its early phase, an unusually fast-decaying transient. The latter phenomenon turned out to be a subtraction artifact, since none of the pharmacological components (L-, N-, P/Q-, and R-type) that constitute the total HVA currents under study showed a similarly fast early decay: hence, the slow activation kinetics of residual currents was not due to the preferential inhibition of a fast-activating/inactivating component, but rather to a true slowing effect of the blocker cations. The percent I_{Ba}-amplitude inhibition caused by Mn^{2+}, Co^{2+}, and Cu^{2+} was voltage-independent over the whole potential range explored (up to +30 mV), hence the slowing of I_{Ba} activation kinetics was not due to a mechanism of voltage- and time-dependent relief from block. Moreover, Mn^{2+}, Co^{2+}, and Cu^{2+} significantly reduced I_{Ba} deactivation speed upon repolarization, which also is not compatible with a depolarization-dependent unblocking mechanism. The above results show that 1) Cu^{2+} is a particularly potent HVA Ca^{2+}-channel blocker in rat palaeocortical neurons; and 2) Mn^{2+}, Co^{2+}, and Cu^{2+}, besides exerting a blocking action on HVA Ca^{2+}-channels, also modify Ca^{2+}-current activation and deactivation kinetics, most probably by directly interfering with channel-state transitions.

Key words: Calcium currents — Copper — Cobalt — Manganese — Block — Activation kinetics — Channel gating — Patch clamp

Introduction

Several divalent metal cations of groups VII*A*-II*B*, including manganese (Mn^{2+}), cobalt (Co^{2+}), nickel (Ni^{2+}), and cadmium (Cd^{2+}) ions, are well known blockers of voltage-gated Ca^{2+} channels (Hagiwara & Nakajima, 1966; Hagiwara & Takahashi, 1967; Hagiwara & Byerly, 1981). These blocker ions have been demonstrated, or are thought, to exert their effects by binding with high affinity to a site located inside the permeation path of voltage-gated Ca^{2+} channels and normally occupied by the permeant ion (Lansman, Hess & Tsien, 1986; Taylor, 1988; Swandulla & Armstrong, 1989; Chow, 1991; Winegar, Kelly & Lansman, 1991; Thévenod & Jones, 1992). In some instances, it has been demonstrated that this binding site coincides with the selectivity filter of the Ca^{2+}-channel pore (e.g., Yang et al., 1993). Mn^{2+} is known to be an example of a partially permeating blocker, in that, besides exerting a blocking effect on Ca^{2+} inflow via the above-described mechanism, under particular conditions it can in turn permeate through Ca^{2+} channels (Delahayes, 1975; Ochi, 1975; Fukuda & Kawa, 1977), thereby producing measurable inward currents (Ochi, 1970; Aimers & Palade, 1981). Ni^{2+} and, especially, Cd^{2+} are potent Ca^{2+}-channel blockers, and have been reported to exert differential effects on different subtypes of voltage-

Correspondence to: J. Magistretti; email: jmlab1@unipv.it

dependent Ca^{2+} currents and channels (reviewed by Bean, 1989; Carbone & Swandulla, 1989). Co^{2+} is also a widely used, although less potent, Ca^{2+}-channel blocker. At the single-channel level, the interactions between these metal ion blockers and the pore of voltage-gated Ca^{2+} channels have been recognized to take place in an "intermediate" or "fast" time scale (see Hille, 2001), thereby producing either a rapid "flickering" of channel openings, or an apparent decrease of unitary-current amplitude (Chesnoy-Marchais, 1985; Lansman et al., 1986; Huang et al., 1989; Winegar et al., 1991).

The effects of copper (Cu^{2+}) ions on neuronal and non-neuronal voltage-gated Ca^{2+} channels are much less characterized. However, differently from most of the above-mentioned divalent metal ions, and similarly to zinc, copper is a trace element of biological relevance, and could physiologically exert modulatory actions on neuronal ion channels. Histological staining techniques reactive for metal cations including Zn^{2+} and Cu^{2+} have revealed that pools of Zn^{2+} and/or Cu^{2+} are stored at high levels and in "free" form in synaptic terminals and vesicles of specific populations of central neurons (Ibata & Otsuka, 1969; Perez-Clausell & Danscher, 1985; Holm et al., 1988; Slomianka, Danscher & Frederickson, 1990; Sato et al., 1994; Schroder et al., 2000). Some evidence also exists that Cu^{2+} contained in synaptic terminals can be released in the extracellular space in an activity-dependent manner (Hartter & Barnea, 1988; Kardos et al., 1989). On the other hand, Cu^{2+} has proven able to affect, at relatively low concentrations, various neuronal ligand- and voltage-gated ion channels, including GABAergic and glutamatergic receptors (Ma & Narahashi, 1993; Narahashi et al., 1994; Kumamoto & Murata, 1995; Weiser & Wienrich, 1996; Trombley & Shepherd, 1996; Vlachova, Zemkova & Vyklicky, 1996), and voltage-dependent K^+ and Na^+ channels (Robbins et al., 1992; Horning & Trombley, 2001), thereby modifying neuronal excitability in multiple ways (Doreulee, Yanovsky & Haas, 1997; Horning & Trombley, 2001).

The effects of group VII*A*-II*B* metal ions on the voltage-dependent and kinetic properties of voltage-gated Ca^{2+} channels are less completely characterized than their blocking actions. In some neuronal preparations, Ni^{2+} has been shown to slow the activation kinetics of voltage-dependent Ca^{2+} currents (McFarlane & Gilly, 1998; Magistretti et al., 2001). The underlying mechanism has been demonstrated to be different from a process of voltage- and time-dependent relief from channel-pore block (Magistretti et al., 2001). A very similar effect is exerted by Zn^{2+} on voltage-dependent Ca^{2+} currents of palaeocortical neurons (Magistretti et al., 2003). Ni^{2+} has also been found to modify the voltage dependence of various voltage-gated Ca^{2+} channels heterologously expressed in *Xenopus* oocytes (Zamponi, Bourinet & Snutch, 1996), with a mechanism different from voltage dependence of binding affinity, and probably implying the interaction with binding site(s) different from those involved in channel-pore block. Effects of other group VII*A*-II*B* ions on Ca^{2+}-channel gating properties have not been reported so far or have not been analyzed in detail.

With the present study we extend our previous work on divalent metal cations and neuronal voltage-gated Ca^{2+} channels (Magistretti et al., 2001, 2003) by analyzing the effects of Cu^{2+}, Co^{2+}, and Mn^{2+} on Ba^{2+} currents conducted through high-voltage-activated (HVA) Ca^{2+} channels in rat piriform-cortex neurons. We report that Cu^{2+} is a potent Ca^{2+}-channel blocker under the experimental conditions here employed. Further, we describe how all three metal ions exert major effects on Ca^{2+}-channel gating properties, resulting in slowing of the activation and deactivation kinetics of the corresponding macroscopic currents. The similarities of the above actions with those already reported for Ni^{2+} and Zn^{2+}, and the biophysical aspects of the underlying mechanistic processes, are also discussed.

Materials and Methods

Cell Preparation

The procedure for isolating pyramidal neurons from rat piriform-cortex layer II has been described in detail elsewhere (Magistretti et al., 2003). Briefly, young (P12–P22) Wistar rats of either sex were decapitated, according to a procedure approved by the University of Pavia Ethical Committee and compliant with the national laws on animal research. The brain was quickly extracted under hypothermic conditions, the two hemispheres were separated, and each was cut with a McIlwain tissue chopper into 350-μm thick quasi-coronal slices, the plane of which was normal to the main axis of the lateral olfactory tract. Layer II of anterior piriform cortex was carefully dissected from each slice under microscopic control. During this operation the slices were submerged in an ice-cold solution composed of (in mmol/l): 115 NaCl, 3 KCl, 3 $MgCl_2$, 0.2 $CaCl_2$, 20 piperazine-N,N′-bis (2-ethanesulphonic acid) · 1.5 Na (PIPES-Na), and 25 D-glucose (pH 7.4 with NaOH, bubbled with pure O_2). Cells were isolated from the layer-II tissue fragments thus obtained by means of an enzymatic (using 1 mg/ml protease type XIV, Sigma, St. Louis, MO) and mechanical dissociation procedure described elsewhere (Magistretti et al., 2003).

Patch-clamp Recordings

The recording chamber was mounted on the stage of an Axiovert 100 microscope (Zeiss, Oberkochen, FRG). The cells were observed at ×400 magnification. After cell seeding, the chamber was perfused with an oxygenated extracellular solution suitable for isolating Ba^{2+} currents conducted through Ca^{2+} channels, containing (in mmol/1): 88 choline-Cl, 40 tetraethylammonium (TEA)-Cl, 3 KCl,

2 $MgCl_2$, 5 $BaCl_2$, 3 CsCl, 10 N-[2-hydroxyethyl] piperazine-N′-[2-ethanesulphonic acid] (HEPES), 5 4-aminopyridine, and 25 D-glucose (pH 7.4 with HCl). Perfusion rate was about 0.5 ml/min. Patch pipettes were fabricated from thick-wall borosilicate glass capillaries (CEI GC 150-7.5; Harvard Apparatus, Edenbridge, UK) by means of a Sutter P-87 horizontal puller (Sutter Instruments, Novato, CA). The pipette solution contained (in mmol/l): 78 Cs methanesulphonate, 40 TEA-Cl, 10 HEPES, 10 ethylene glycol-bis (β-aminoethyl ether) N,N,N′,N′-tetraacetic acid (EGTA), 20 phosphocreatine di-Tris salt, 2 adenosine 5′-triphosphate-Mg, 0.2 guanosine 5′-triphosphate-Na, and 20 U/ml creatinephosphokinase (pH adjusted to 7.2 with CsOH). The patch pipettes had a resistance of 3–5.5 MΩ when filled with the above solution. Tight seals (>10 GΩ) and the whole-cell configuration were obtained according to the standard technique (Hamill et al., 1981). Voltage-clamp recordings of Ba^{2+} or Ca^{2+} currents were performed at room temperature (~22°C) by means of an EPC7 patch-clamp amplifier (List Electronics, Darmstadt, FRG). After the establishment of the whole-cell condition, voltage-dependent currents were allowed to stabilize for a few minutes before starting data acquisition. Series resistance (R_s) was evaluated on line by canceling the whole-cell capacitive transients evoked by −5-mV square voltage pulses with the amplifier's compensation section, and reading out the corresponding values. R_s averaged 9.1 ± 0.6 MΩ ($n = 35$), was always compensated by 50–70%, and was continually monitored during the experiment. Recordings in which R_s levels varied with time by more than 2 MΩ were discarded. Voltage protocols were commanded and current signals were acquired with a Pentium personal computer interfaced to an Axon TL-1 interface, using the Clampex program of the pClamp 6.0.5 software package (Axon Instruments). In all recordings the general holding potential was −70 mV. Unless otherwise specified, every test voltage protocol was preceded by a 2-s conditioning prepulse at −60 mV. Current signals were filtered at 5 kHz, digitized at 100 kHz (tail protocols) or 50 kHz (other protocols), and online leak-subtracted *via* a P/4 protocol.

Drug Application

$MnCl_2$, $CoCl_2$, and $CuCl_2$ (Sigma) and organic Ca^{2+}-channel blockers were applied through a local-perfusion system consisting of a multibarrel pipette (diameter at the tip ~150 μm), each barrel of which was connected to a separate perfusion channel. Upon opening of each channel, controlled by operating remote-commanded electrovalves (Sirai, Milano, Italy), the drug-containing solution flowed by gravity, thus forming a laminar-flux cone. The tip of the perfusion pipette was positioned in close proximity of the recording site, so that the recorded cell was fully drenched by the laminar-flux cone.

Concentrated stock solutions of organic Ca^{2+}-channel blockers were prepared, divided in small aliquots, and stored at −20°C. Nifedipine (Sigma) was dissolved in dimethylsulfoxide (DMSO) at 10 mmol/l; ω-conotoxin GVIA (ω-CTx GVIA), ω-conotoxin MVIIC (ω-CTx MVIIC), and ω-agatoxin IVA (ω-AgaTx IVA) (all from Bachem, Bubendorf, Switzerland) were dissolved in pure water at 1, 1, and 0.1 mmol/l, respectively. The aliquots were then diluted to the final concentrations in the recording solution described in the previous paragraph. ω-CTx MVIIC and ω-AgaTx IVA aliquots were dissolved in the presence of lysozyme (Sigma; 1 mg/ml), in order to minimize aspecific binding to recipient walls. The solvents and additional substances used for each drug (DMSO and lysozyme) were also added, in the same amounts, to the control solution and the other drug-containing solutions used in the same experiment. Due to the drug's light sensitivity, nifedipine was prepared and stored in the dark, and the perfusion channel containing nifedipine was light-shielded.

Data Analysis

Current traces were analyzed by means of the Clampfit program of pClamp 6.0.5. Voltage-clamp conditions were evaluated off-line by analyzing the kinetics of capacitive current transients elicited by −10-mV voltage square pulses. Exponential fittings of capacitive-transient decay returned an average time constant of 155.2 ± 7.7 μs ($n = 31$). This value coincides with the average time constant of the voltage clamp operating inside the cell in the absence of R_s compensation. Activation of R_s compensation to the percentages normally achieved (50–70%: *see* above) allowed for even higher (by ~2–3 times) clamp speed.

Ba^{2+} and Ca^{2+} currents were normally re-filtered off-line at 3 kHz, unless preservation of high-frequency signal components was required (i.e., when tail currents were analyzed). Current amplitude was always measured at the peak of each trace. Data fittings with exponential functions, $I = \Sigma A_i \cdot \exp(-t/\tau_i) + C$, were carried out using Clampfit. Dose-response plots were normally fitted with a single Langmuir adsorption isotherm function, in the form:

$$f_i = [I_{Ba}(C) - I_{Ba}(Me^{2+})]/I_{Ba}(C) = [Me^{2+}]^n/(IC_{50}^n + [Me^{2+}]^n), \quad (1)$$

where f_i is fractional inhibition, $I_{Ba}(C)$ and $I_{Ba}(Me^{2+})$ are the current amplitudes in control conditions and under the divalent metal cation, respectively; IC_{50} is the cation's concentration corresponding to 50% I_{Ba} block, and n is the Hill coefficient. A double Langmuir function was also used in some cases:

$$f_i = \bar{A}_1 \cdot [Me^{2+}]^{n_1}/(IC_{50_1}^{n_1} + [Me^{2+}]^{n_1}) + (1 - \bar{A}_1) \cdot [Me^{2+}]^{n_2}/(IC_{50_2}^{n_2} + [Me^{2+}]^{n_2}), \quad (2)$$

with $0 \le \bar{A}_1 < 1$. Langmuir fittings were performed using Origin 6.0 (MicroCal Software, Northampton, MA). Average values were expressed as mean ± SEM. Statistical significance was evaluated by means of the two-tail Student's t-test for paired data.

Results

Blocking Effects of Mn^{2+}, Co^{2+}, and Cu^{2+} on HVA I_{Ba} in Rat Piriform-Cortex Neurons

Voltage-dependent Ba^{2+} currents (I_{Ba}) were routinely elicited by delivering 50-ms depolarizing steps starting from 2-s prepulses at −60 mV, which allowed for recording of HVA currents in isolation (*see* Magistretti de Curtis, 1998). The effects of Mn^{2+}, Co^{2+}, and Cu^{2+} on I_{Ba} thus recorded in pyramidal neurons acutely isolated from rat piriform-cortex (PC) layer II were first examined by analyzing the blocking action of the three cations. Submillimolar levels of Mn^{2+}, Co^{2+}, and Cu^{2+} were able to block HVA currents in a concentration-dependent manner (Fig. 1*A*). The blocking effect of Mn^{2+} and Co^{2+} was partly reversible (by ~60% and ~45%, respectively) after a 2–5 min washout, whereas that of Cu^{2+} appeared largely nonreversible after the same washout period. The concentration dependence of block was different for the three cations, as revealed by average plots of I_{Ba} fractional inhibition (measured at the peak of the

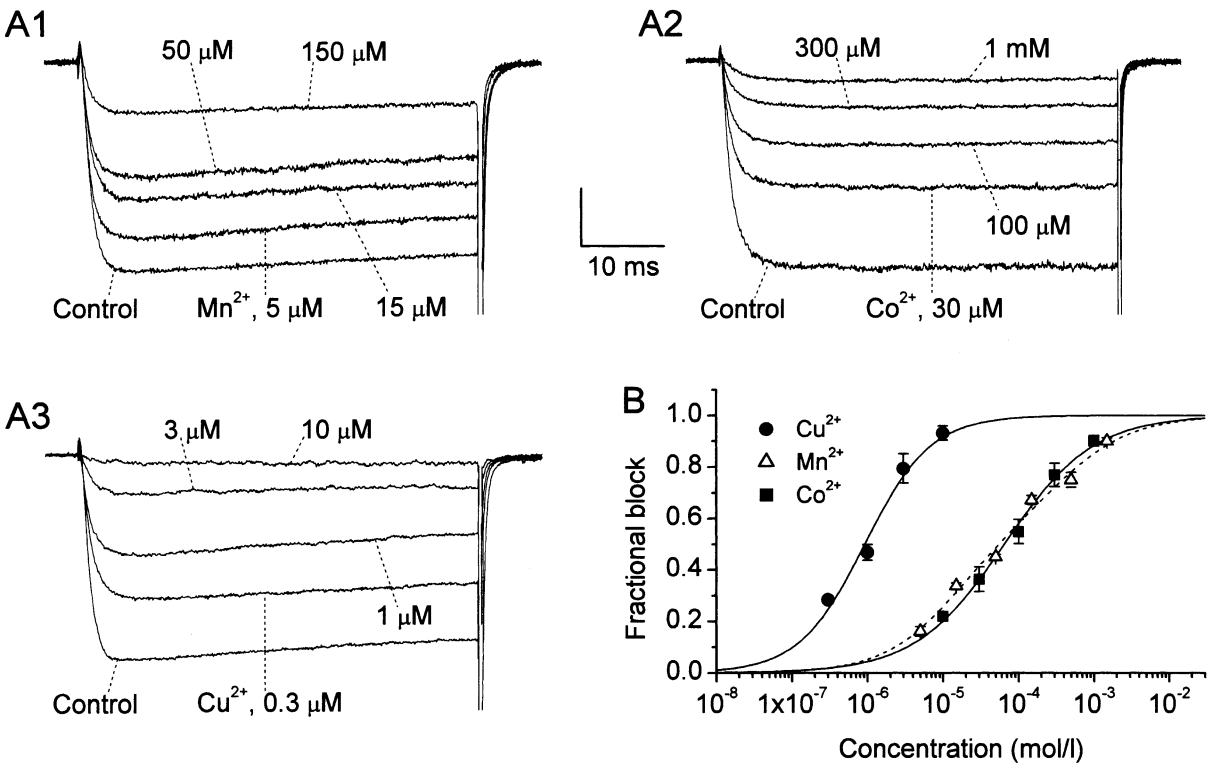

Fig. 1. Concentration dependence of HVA I_{Ba} block by Mn^{2+}, Co^{2+}, and Cu^{2+} in piriform-cortex layer-II pyramidal neurons. (*A*) Effects of increasing concentrations of Mn^{2+} (*A1*), Co^{2+} (*A2*), and Cu^{2+} (*A3*) on HVA currents evoked by 50-ms depolarizing pulses from −60 mV to 0 mV in three representative neurons (cells C2612 in *A1*, A2523 in *A2*, B2604 in *A3*). *Y*-Axis scale: 250 pA (*A1*), 230 pA (*A2*), 335 pA (*A3*). (*B*) Average concentration-dependence plots of I_{Ba} block induced by Mn^{2+} (*empty triangles*), Co^{2+} (*filled squares*), and Cu^{2+} (*filled circles*). Fractional block was measured considering peak values of control currents and residual currents recorded in the presence of each blocking cation. Numbers of observations are: Mn^{2+}, 7 (5–150 μM), 4 (500 and 1500 μM); Co^{2+}, 4 (10 μM), 7 (30 and 300 μM), 9 (100 μM), 6 (1000 μM); Cu^{2+}, 4 (0.3 and 10 μM), 8 (1 μM), 6 (3 μM). Note the logarithmic scale of the *x* axis. Fittings obtained by applying a single Langmuir isotherm function (*smooth, continuous lines*) to each data set returned the following parameters: IC_{50} = 916.9 nM, n = 1.0 (Cu^{2+}); IC_{50} = 57.7 μM, n = 0.61 (Mn^{2+}); IC_{50} = 64.6 μM, n = 0.74 (Co^{2+}). The smooth, dotted line is the fitting obtained by applying a double Langmuir function to Mn^{2+} data, which returned: $\bar{A}_1 = 0.53$, IC_{50_1} = 13.0 μM, n_1 = 0.89, IC_{50_2} = 340.3 μM, n_2 = 0.82.

current-voltage relationship, *I-V*, and considering peak I_{Ba} amplitudes) as a function of blocker concentration (Fig. 1*B*). Data fittings obtained by applying single Langmuir functions (Eq. 1; continuous lines in Fig. 1*B*) returned IC_{50} values of ∼920 nM for Cu^{2+}, ∼58 μM for Mn^{2+}, and ∼65 μM for Co^{2+}. The n coefficient was ∼1.0 in the case of Cu^{2+}, which suggests that Cu^{2+}-dependent block depends on the binding of Cu^{2+} ions to a single binding site within each Ca^{2+} channel, with homogeneous affinity for all of the Ca^{2+} channels expressed by the neurons under study. By contrast, n was clearly lower than 1 in the cases of Co^{2+} and Mn^{2+} (∼0.74 and ∼0.61, respectively). This could imply that Co^{2+} and Mn^{2+} ions interact with distinct subpopulations of HVA channels with different affinities, and, therefore, that the concentration dependence of Mn^{2+} and Co^{2+} block could be better described by the sum of more than one Langmuir function, each with a different IC_{50}. Indeed, the dose-response plot for Mn^{2+}, in which the deviation from 1 of the Hill coefficient obtained by applying a single Langmuir function was greatest, could be successfully fitted with a double Langmuir function (Eq. 2; Fig. 1*B*, dotted line), which returned two IC_{50}s of ∼13 μM and ∼340 μM.

Slow Activation Kinetics of Residual I_{Ba} in the Presence of Mn^{2+}, Co^{2+}, and Cu^{2+} Block

Residual HVA currents recorded during block by Mn^{2+}, Co^{2+}, and Cu^{2+} at submaximal concentrations appeared to activate with substantially slower kinetics than control currents. This is illustrated in Fig. 2*A–C* where control I_{Ba} and residual I_{Ba}, recorded in the presence of 150 μM Mn^{2+}, 300 μM Co^{2+}, 1 μM Cu^{2+}, and 3 μM Cu^{2+}, are shown, over an expanded time scale, normalized to their maximal amplitudes. Residual currents reached their peak with a clearly slower time course than control currents. Also in the presence of 5 μM Cd^{2+}, which reduced I_{Ba} amplitude by 84.4 ± 1.4% (n = 3), residual currents

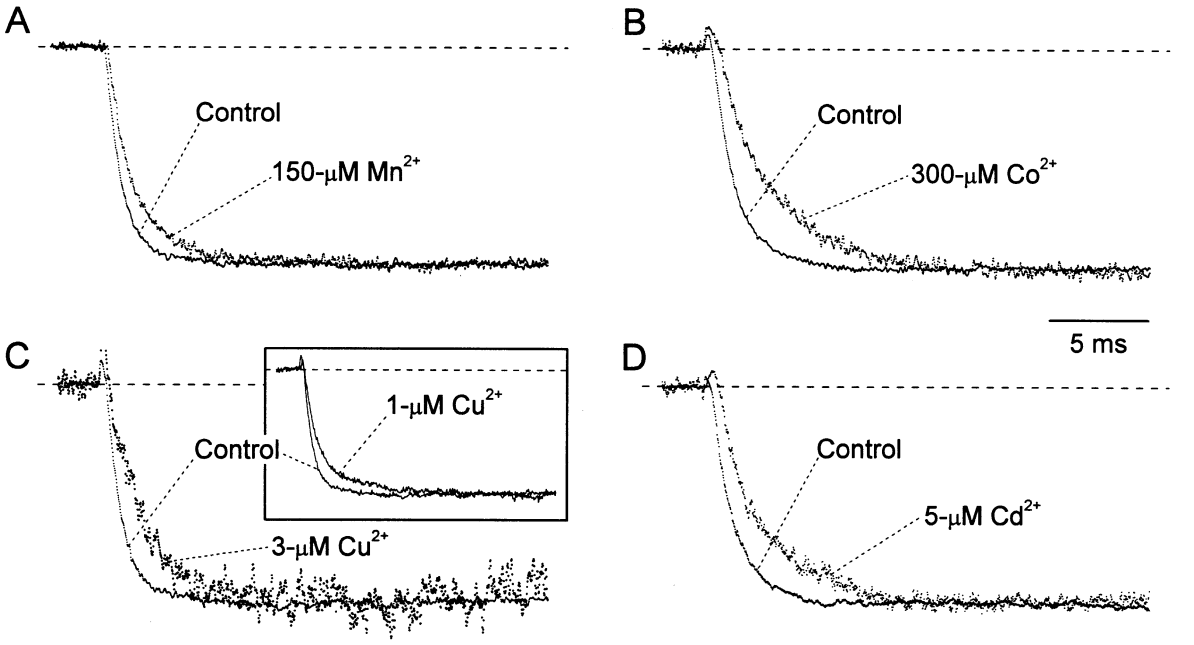

Fig. 2. Slow activation kinetics of residual I_{Ba} in the presence of Mn^{2+}, Co^{2+}, Cu^{2+}, and Cd^{2+} block. Currents were evoked with depolarizing pulses from −60 mV to 0 mV in four different, representative neurons (cells A2620 in *A*, A2524 in *B*, A2605 in *C*, A1227 in *D*), in control conditions and in the presence of 150 μM Mn^{2+}, 300 μM Co^{2+}, 3 μM (main panel) or 1 μM (inset) Cu^{2+}, and 5 μM Cd^{2+}. The currents are shown normalized to their peak amplitudes over an expanded time scale. Note that the traces are depicted as separate points to highlight the high temporal resolution of the acquisition.

activated with markedly slower kinetics than control currents (Fig. 2*D*).

To quantify the above effects, exponential fittings of the activation phases of I_{Ba} evoked at various test potentials (−30 to +30 mV)[1] were performed (Fig. 3*A*). The activation kinetics of the currents under study were normally biexponential. Fitting parameters were used to derive a lumped, or overall, activation time constant ($\bar{\tau}_{act}$; *see* Magistretti et al., 2001):

$$\bar{\tau}_{act} = \tau_{act1} \cdot A_1/(A_1 + A_2) + \tau_{act2} \cdot A_2/(A_1 + A_2). \quad (3)$$

In all cases, $\bar{\tau}_{act}$ was significantly higher in residual currents than in control currents. At 0 mV (the peak of *I-V* plots: *see* below), $\bar{\tau}_{act}$ was increased on average by 50.2 ± 10.8% in the presence of 150 μM Mn^{2+} (n = 5); 65.4 ± 11.0% in 300 μM Co^{2+} (n = 7); 57.6 ± 13.6% in 1 μM Cu^{2+} (n = 8); 86.4 ± 11.9% in 3 μM Cu^{2+} (n = 5); and 124.0 ± 36.7% in 5 μM Cd^{2+} (n = 3). $\bar{\tau}_{act}$ values of residual currents were significantly increased in a wide range of test potentials (Fig. 3*B*). Percent $\bar{\tau}_{act}$ increases observed between −10/−20 mV and +30 mV averaged ~20 to 50% for 150 μM Mn^{2+}; ~50 to 70% for 300 μM Co^{2+}; ~50 to 60% for 1 μM Cu^{2+}; and ~80 to 130% for 3 μM Cu^{2+}.

The so far described effects of divalent metal cations on HVA currents were observed in the presence of 5 mM Ba^{2+} as the permeant cation. One might wonder whether similar effects would also be found in the presence of physiological concentrations of Ca^{2+}. This issue has special importance in the case of Cu^{2+}, which, differently from the other here investigated cations, is likely to play some physiological role(s) in neurotransmission and/or neuromodulation (*see* Introduction). We therefore tested the effects of Cu^{2+} on the HVA currents recorded in the presence of 1 mM Ca^{2+} as the charge carrier (Fig. 4). Under these conditions, 1 μM Cu^{2+} reduced HVA current amplitude by 41.4 ± 6.9% (n = 5), as compared to 46.8 ± 3.1% (n = 8) in 5 mM Ba^{2+}. Activation kinetics of residual currents also appeared to be slower than in control currents (*see* Fig. 4, lower traces). At 0 mV, $\bar{\tau}_{act}$ was higher, on average, by 53.6 ± 10.5% (n = 5) in currents recorded in the presence of 1 μM Cu^{2+} than in control currents. Hence, the here investigated actions of metal cations on HVA currents appeared to be similar when using either 5 mM extracellular Ba^{2+} or Ca^{2+} at nearly physiological concentrations. The experiments illustrated from this point on were performed using 5 mM Ba^{2+} as the charge carrier, which considerably increased current amplitude and improved recording stability.

[1]Currents recorded at voltages positive to 0 mV occasionally showed signs of contamination by small, unblocked outward currents. Therefore, the currents used for this type of analysis and for constructing *I-V* relationships (*see* Fig. 6), as well as those obtained with action potential-like waveforms (*see* Fig. 9), were always corrected by subtraction of from the currents recorded after application of a saturating concentration (200 μM) of Cd^{2+}.

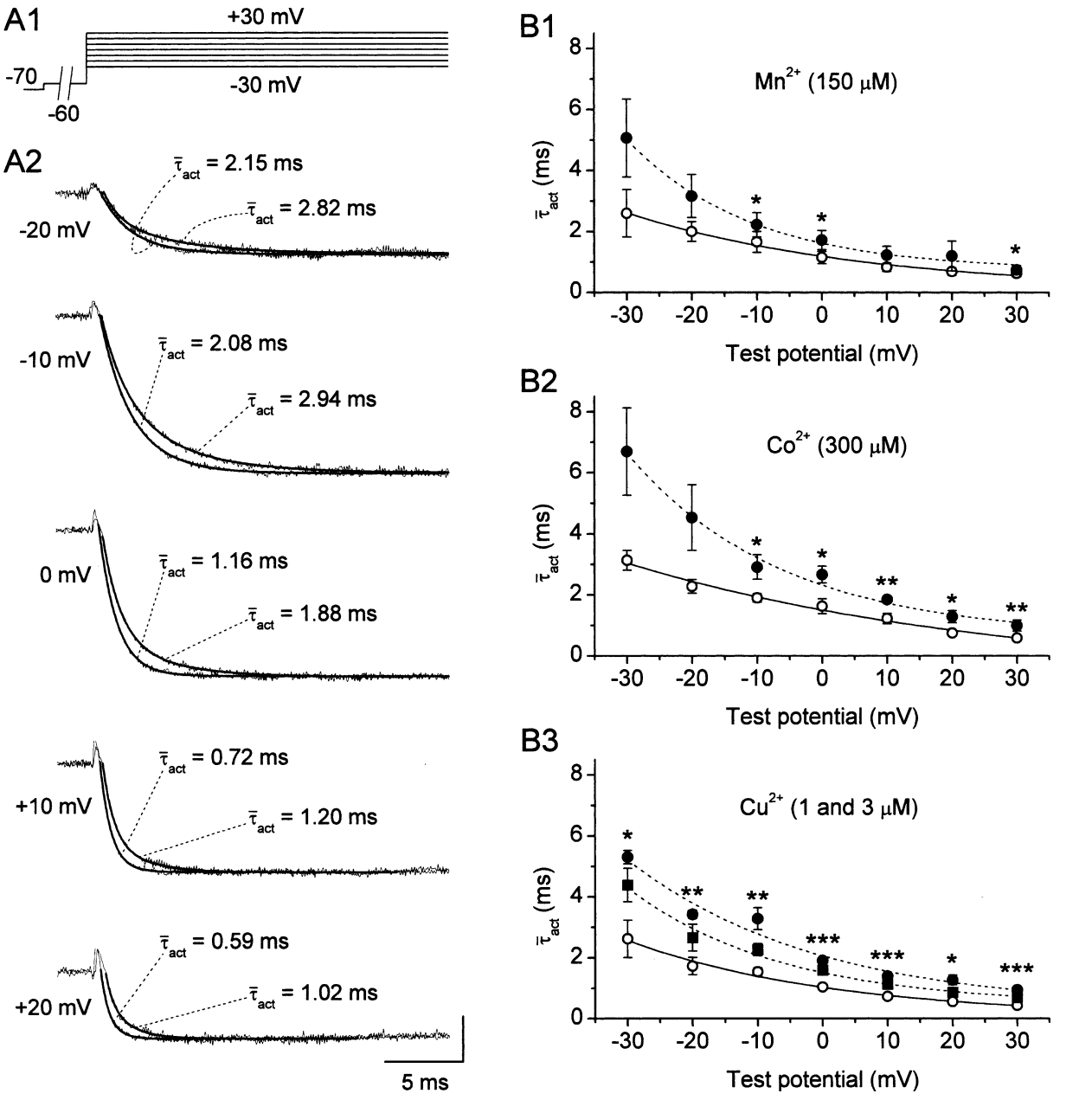

Fig. 3. Analysis of the effects of Mn^{2+}, Co^{2+}, and Cu^{2+} on I_{Ba} activation kinetics. (*A*) Detail of the activation phases of I_{Ba} recorded in a representative neuron (cell B2610) in response to step depolarizations at various voltage levels (*see* the voltage protocol in *A1*), before and during application of 1 μM Cu^{2+}. All currents are Cd^{2+}-subtracted and have been normalized to their peak amplitudes. The slower-activating currents are those recorded in the presence of Cu^{2+}. Enhanced lines are biexponential best fittings to current activation phases. The values of the lumped activation time constant ($\bar{\tau}_{act}$; *see* text for details) are also indicated. *Y*-Axis scale (for control currents only): 200 pA. (*B*) Average plots of the voltage dependence of $\bar{\tau}_{act}$, as calculated from the parameters returned by biexponential fittings of the I_{Ba} activation phase. *Empty circles, continuous lines:* control; *filled circles, dotted lines*: 150 μM Mn^{2+} (*B1*), 300 μM Co^{2+} (*B2*), and 3 μM Cu^{2+} (*B3*); *filled squares* in (*B3*): 1 μM Cu^{2+}. ***, $p < 0.001$; **, $p < 0.01$; *, $p < 0.05$ (*t*-test for paired data). Asterisks in panel *B3* refer to data on 3 μM Cu^{2+}; levels of significance for 1 μM Cu^{2+} were the same as for 3 μM Cu^{2+}, except at −20 mV ($p < 0.05$), 0 and +10 mV ($p < 0.01$ in both cases), $n = 4$ (Co^{2+}) and 5 (Mn^{2+}, Cu^{2+}).

Slowing of Residual I_{Ba} Activation Kinetics in the Presence of Mn^{2+}, Co^{2+} and Cu^{2+} Is not Due to Selective Block of Fast-activating Current Component(s)

The slow activation kinetics observed in the residual currents recorded during application of Mn^{2+}, Co^{2+}, and Cu^{2+} can, in principle, be explained in two different ways: 1) the divalent metal cations preferentially block a fast-activating current component, thus revealing an underlying slower-activating current; 2) the divalent metal cations actually reduce the activation speed of whole-cell I_{Ba}, with a mechanism to be determined. To test the former hypothesis, we

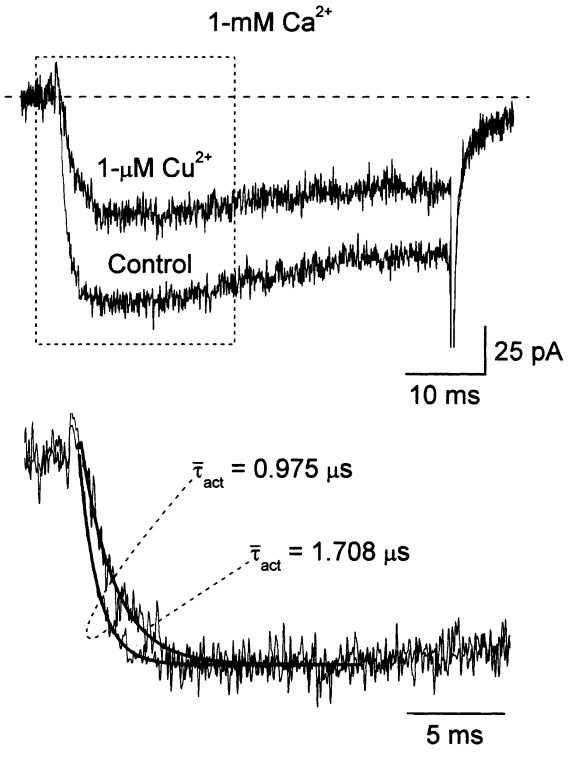

Fig. 4. Effects of 1 μM Cu^{+} on HVA currents in the presence of 1 mM Ca^{2+} as the charge carrier. The upper traces are Ca^{2+} currents recorded in response to 50-ms depolarizing pulses from −60 mV to 0 mV in a representative neuron (cell B3523), before and during application of 1 μM Cu^{2+}. The lower traces correspond to the early part of the currents shown in the upper panel (dotted-line box): here currents have been normalized to their peak amplitudes to highlight their different activation kinetics (the slower-activating current is the residual current in the presence of Cu^{2+}). Enhanced lines are biexponential best fittings to current activation phases. The values of the lumped activation time constant ($\bar{\tau}_{act}$; *see* text for details) are also indicated.

compared the currents sensitive to Mn^{2+}, Co^{2+}, and Cu^{2+} block, isolated by subtraction, with the single pharmacological components in which the total I_{Ba} under study can be dissected. The slow time course of residual-current activation in the presence of submaximal concentrations of Mn^{2+}, Co^{2+}, and Cu^{2+} was such that Mn^{2+}-, Co^{2+}-, and Cu^{2+}-sensitive currents, obtained by subtraction, frequently showed an early phase characterized by fast inactivation (Fig. 5*A* and *B*, *arrows*). The decay time constant of this early current transient was typically <8.04 ms. The currents thus obtained were compared with the L-, N-, P/Q, and R-type current fractions that can be isolated from total I_{Ba} using specific Ca^{2+}-channel blockers. Saturating concentrations of nifedipine (1 μM), ω-CTx GVIA (1 μM), and ω-AgaTx IVA (100 nM) were used to isolate, by subtraction, the L-, N-, P/Q-type currents, respectively. The R-type current component was isolated by simultaneously applying 10 μM nifedipine, 1 μM ω-CTx GVIA, and the N- and P/Q-channel blocker, ω-CTx MVIIC (1 μM). As exemplified in Fig. 5*C*, with none of the above pharmacological components an early, fast-inactivating transient similar to that typically observed in Mn^{2+}-, Co^{2+}-, and Cu^{2+}-sensitive currents obtained by subtraction was seen. L-, N-, P/Q-type currents were barely inactivating or largely non-inactivating during the routinely applied 50-ms pulses (Fig. 5*C1–3*) (n = 6, 5, and 4, respectively). Only the R-type component showed a more prominent tendency to inactivate (Fig. 5*C4*) but with time constants much higher (42.5 ± 8.7 ms at 0 mV, n = 6) than those characterizing the early transients of Mn^{2+}-, Co^{2+}-, and Cu^{2+}-sensitive currents. These observations indicate that the slow time course of residual-current activation in the presence of Mn^{2+}, Co^{2+}, and Cu^{2+} is not due to the preferential inhibition of a specific, fast-activating and -inactivating current component by the same metal cations. Once this possibility has been ruled out, we can conclude that the same metal cations exert a real slowing effect on I_{Ba} activation kinetics, and that the fast inactivation phase observed in blocker-sensitive currents is actually a subtraction artifact.

Mn^{2+}-, Co^{2+}-, and Cu^{2+}-Induced Slowing of I_{Ba} Activation Kinetics: Analysis of the Mechanism of Action

As discussed in more detail elsewhere for the specific case of Ni^{2+} (Magistretti et al., 2001), a slowing effect exerted by an extracellular blocking cation on the activation phase of voltage-dependent Ca^{2+} currents could, in principle, be due to an intrinsic voltage dependence of Ca^{2+}-channel block: if, upon depolarization, the block is partly relieved with relatively slow kinetics, the unblocking process could produce an apparent decrease of the activation speed of residual currents. Under the hypothesis that this mechanism applies to the here studied cases of Mn^{2+}, Co^{2+}, and Cu^{2+}, the steady-state blocking effect of the same cations on I_{Ba} would be expected to be progressively smaller with increasingly positive voltage levels of the pulses used to elicit I_{Ba} itself. To test this possibility, the voltage-dependence of Mn^{2+}, Co^{2+}, and Cu^{2+} block was examined by analyzing *I-V* plots of control and residual I_{Ba} (Fig. 6). The shape and position over the x axis of average *I-V* relationships was not modified by increasing concentrations of Mn^{2+}, Co^{2+}, and Cu^{2+} (Fig. 6*A1*, *B1*, *C1*). This appeared particularly evident when *I-V* plots were normalized for their maximal amplitude, which revealed an almost exact overlap between the *I-V*s of residual currents and control *I-V*s (Fig. 6*A2*, *B2*, *C2*). Hence, Mn^{2+}, Co^{2+}, and Cu^{2+} block of total I_{Ba} is not voltage-dependent over the examined voltage range of I_{Ba} activation.

To conclusively demonstrate that the slower activation kinetics observed in residual currents after

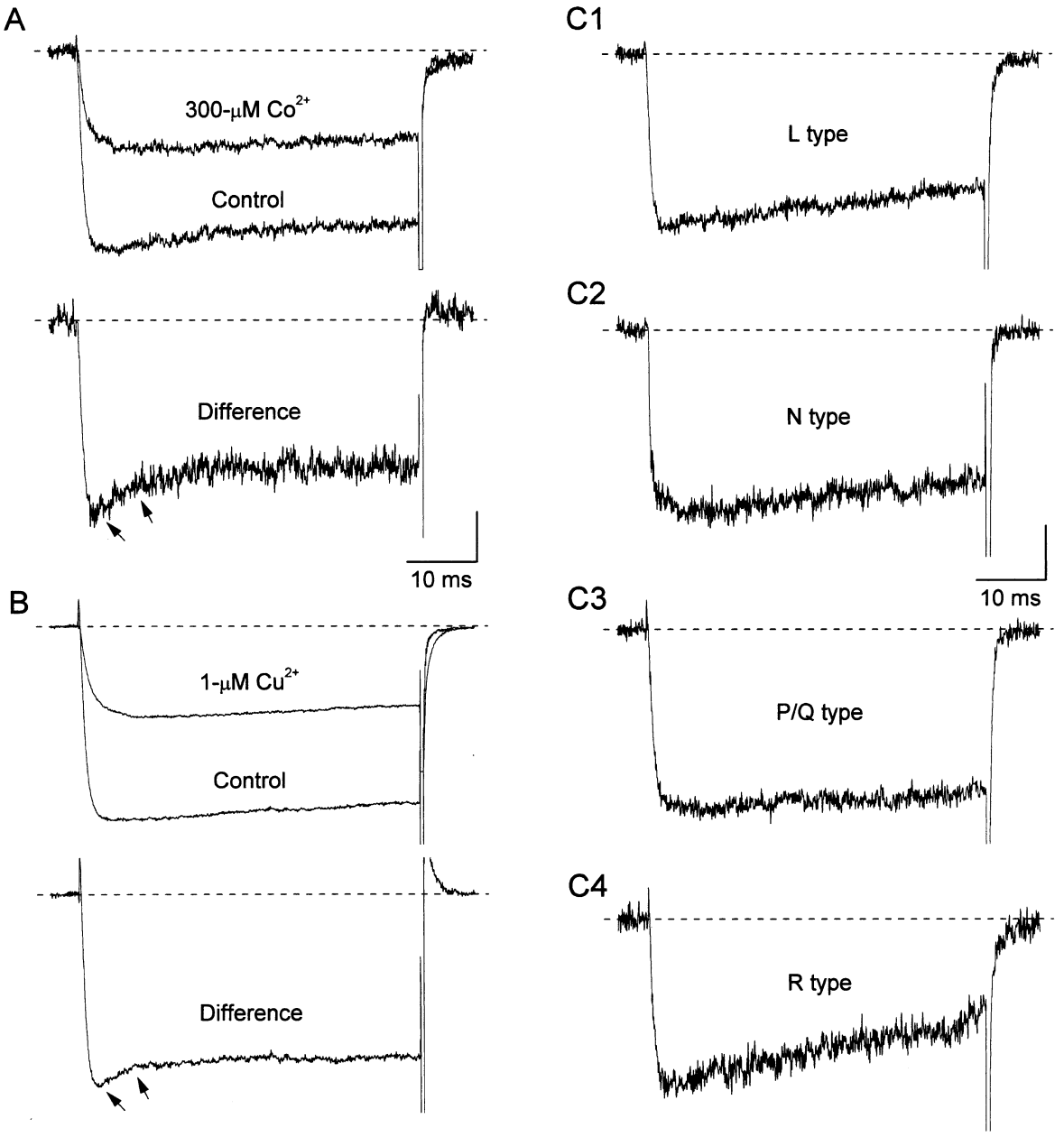

Fig. 5. I_{Ba} fractions abolished by submaximal concentrations of divalent metal cations display markedly different time courses in their early phases as compared to L-, N-, P/Q-, and R-type current components. (*A*) *Top traces*: I_{Ba} recorded in a representative neuron (cell C2527) in response to step depolarizations from −60 mV to 0 mV before and during application of 300 μM Co^{2+}. *Bottom trace*: the current fraction abolished by Co^{2+} obtained by subtraction. *Y*-Axis scale: 70 pA (*top*), 40 pA (*bottom*). (*B*) *Top traces*: I_{Ba} recorded in a representative neuron (cell C2604) before and during application of 1 μM Cu^{2+}. *Bottom trace:* the current fraction abolished by Cu^{2+}. *Y*-Axis scale: 350 pA (*top*), 210 pA (*bottom*). The arrows in *A* and *B* point to the fast-decaying, early transient present in the current fractions abolished by metal cations. (*C*) L-, N-, P/Q-, and R-type I_{Ba} components isolated in four different neurons using 10 μM nifedipine (*C1*), 1 μM ω-CTx GVIA (*C2*), 1 μM ω-AgaTx IVA (*C3*), and 10 μM nifedipine + 1 μM ω-CTx GVIA + 1 μM ω-CTx MVIIC (*C4*), respectively. *Y*-Axis scale: 106 pA (*C1* and *C3*), 50 pA (*C2*), 27 pA (*C4*).

Mn^{2+}, Co^{2+}, and Cu^{2+} block is not due to a mechanism of slow relief from an intrinsically voltage-dependent block upon depolarization, it is necessary to exclude that such an unblocking process is complete and saturating between −60 mV (the usual pre-step level) and −30 mV (the first voltage level at which sizeable I_{Ba} starts to be recorded) (*see* Magistretti et al., 2001, for more details on this issue). Under the latter hypothesis, no cation-dependent slowing of residual-current activation kinetics should be observed when delivering depolarizing test pulses from −30 mV rather than from the usual pre-step level of −60 mV. To test this possibility, we performed experiments in which I_{Ba} was evoked, both in

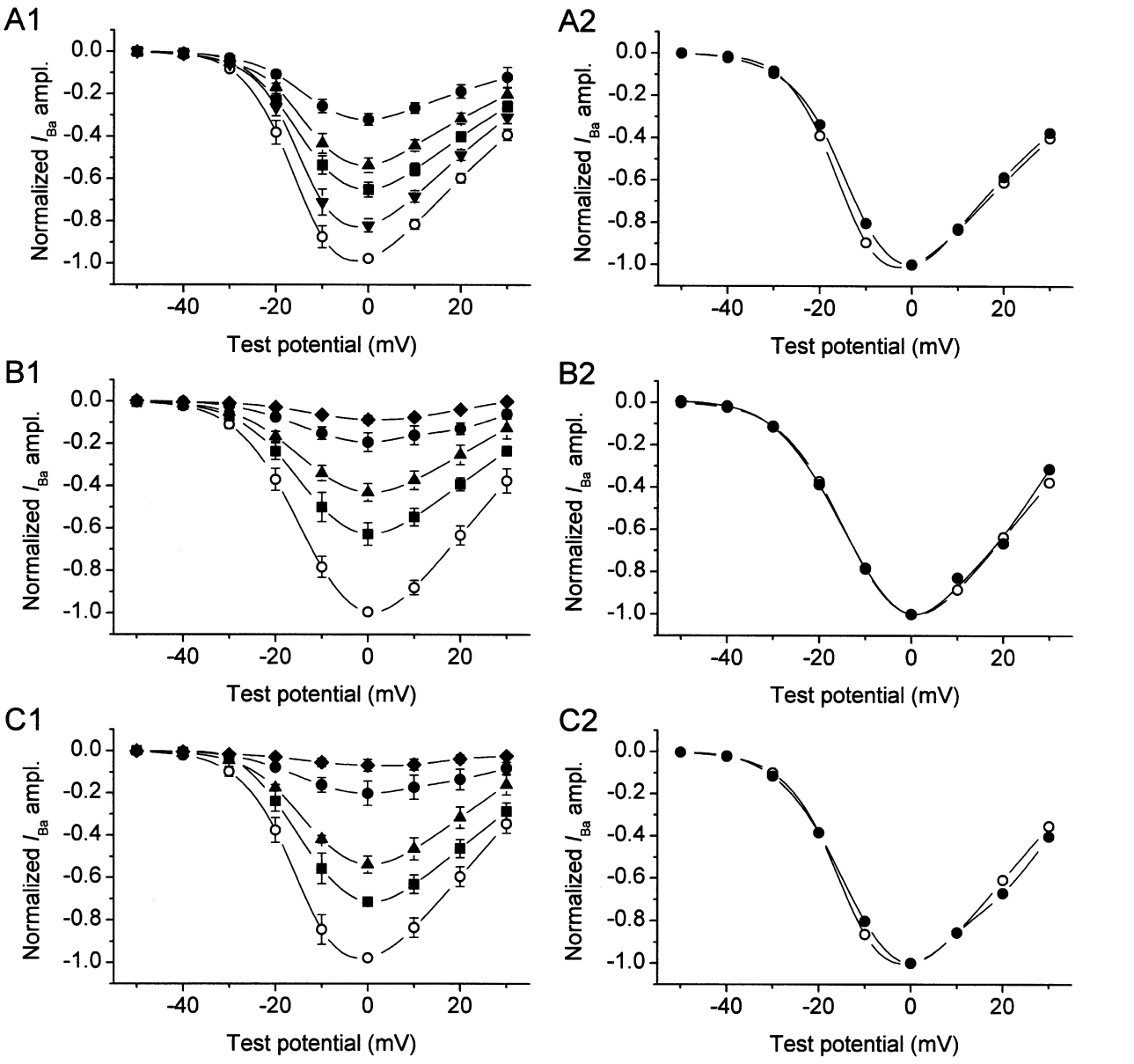

Fig. 6. Mn^{2+}, Co^{2+}, and Cu^{2+} do not modify the current-voltage relationship of HVA I_{Ba}. The figure shows average *I-V* plots of control currents and residual currents recorded during application of various concentrations of Mn^{2+} (*A*), Co^{2+} (*B*), and Cu^{2+} (*C*). All currents used for this analysis were Cd^{2+}-subtracted. The *I-V*s of each cell were normalized for the maximal current value observed in control conditions, then *I-V*s were averaged among cells. Left panels show the *I-V*s thus obtained in control conditions (*empty circles*) and in the presence of increasing concentrations of Mn^{2+} (5, 15, 50, and 150 μM; *A1*), Co^{2+} (30, 100, 300, and 1000 μM; *B1*), and Cu^{2+} (0.3, 1, 3, and 10 μM; *C1*). Right panels show control *I-V*s (*empty circles*) and *I-V*s obtained with 150 μM Mn^{2+} (*A2*), 300 μM Co^{2+} (*B2*), and 3 μM Cu^{2+} (*C2*): here the *I-V* plots have been normalized for the maximal value of each, to highlight the overlap of their shape and position along the *x* axis. Numbers of observations are: Mn^{2+}, 7 (control and 50 μM), 6 (5, 15 and 150 μM); Co^{2+}, 9 (control and 100 μM), 6 (30 and 300 μM), 5 (1000 μM); Cu^{2+}, 6 (control, 1 and 3 μM), 4 (0.3 and 10 μM).

control conditions and in the presence of 150 μM Mn^{2+}, 300 μM Co^{2+}, or 3 μM Cu^{2+}, by test pulses at 0 mV, delivered either from the usual level of −60 mV, or after a conditioning prepulse at −30 mV (Fig. 7*A1*). The duration of this prepulse was 25 ms, namely ∼6 times the average $\bar{\tau}_{act}$ observed, at the same voltage, in residual currents during application of the same concentrations of the three cations (*see* Fig. 3*B*). The normalized currents of Fig. 7*A2* and *A3* clearly show that an evident slowing of residual-current activation kinetics was still present even after the prepulse at −30 mV. Fig. 7*B1–B3* illustrates average $\bar{\tau}_{act}$ values measured in control currents (*white bars*) and during Mn^{2+}, Co^{2+}, and Cu^{2+} block (*hatched bars*), both in the absence and in the presence of the prepulse at −30 mV. In no case was the

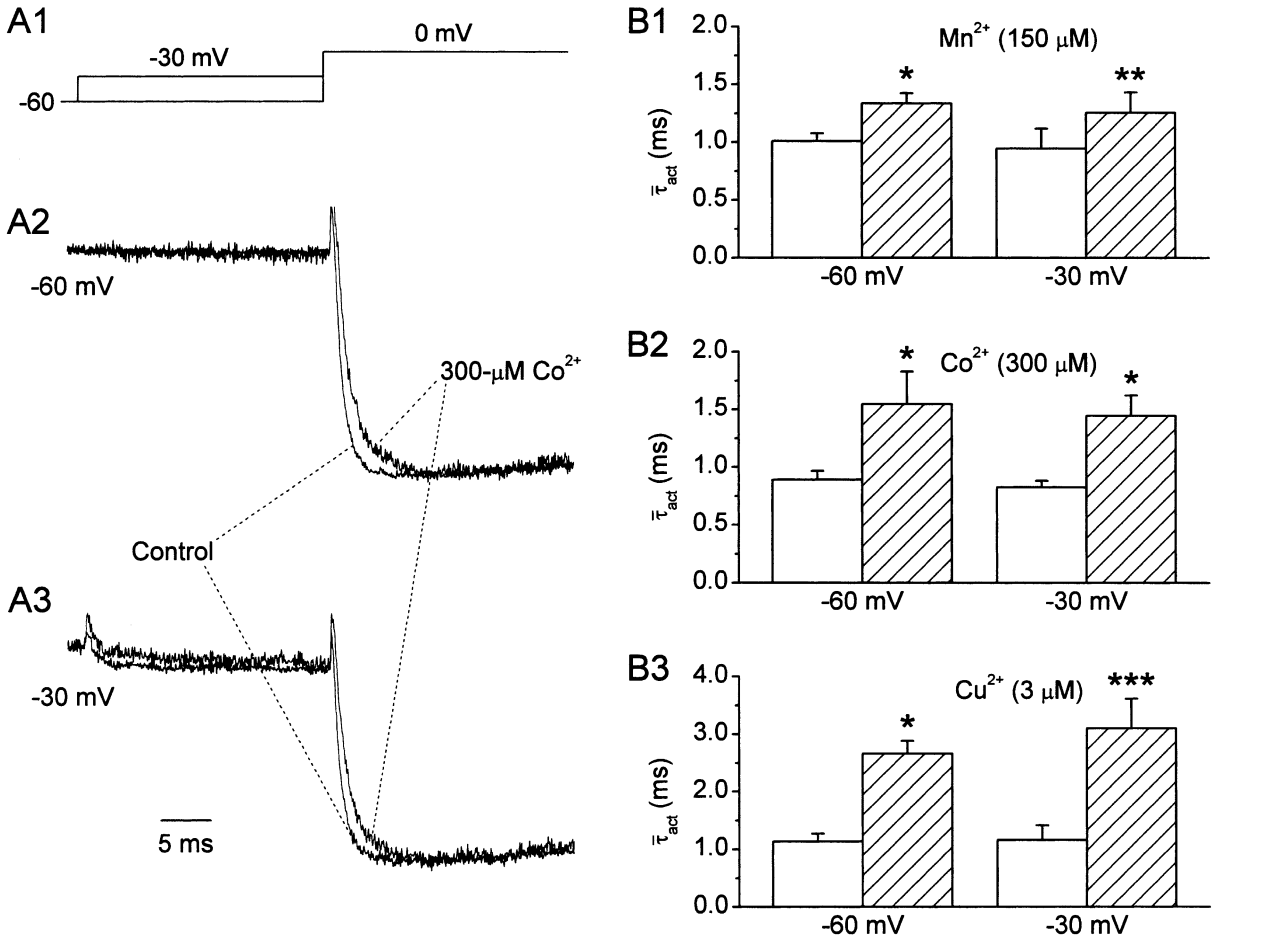

Fig. 7. Slowing of residual I_{Ba} during application of Mn^{2+}, Co^{2+}, and Cu^{2+} is not affected by depolarizing prepulses at −30 mV. (*A*) The experimental protocol used for testing the effect of depolarizing pre-steps on the slowing of I_{Ba} activation kinetics induced by divalent metal cations. Panel *A1* illustrates the voltage protocol applied, panels *A2* and *A3* show the I_{Ba} thus recorded in a representative neuron (cell A2N15) in control conditions and during application of 300 μM Co^{2+}, in the absence (*A2*) and in the presence (*A3*) of the 25-ms prepulses at −30 mV. Currents have been normalized to their peak values. (*B*) Average $\bar{\tau}_{act}$ values measured in control currents (*white bars*) and during application of 150 μM Mn^{2+} (*B1*), 300 μM Co^{2+} (*B2*), and 3 μM Cu^{2+} (*B3*) (*hatched bars*), both in the absence and in the presence of the prepulse at −30 mV. ***, $p < 0.001$; **, $p < 0.01$; *, $p < 0.05$ (*t*-test for paired data). $n = 3$ (Mn^{2+}, Cu^{2+}) and 7 (Co^{2+}).

percent $\bar{\tau}_{act}$ increase caused by the three blocking cations significantly modified by the pre-step depolarization ($p > 0.55$ in all cases). Taken together, the above results demonstrate that the decrease in I_{Ba} activation speed carried out by Mn^{2+}, Co^{2+}, and Cu^{2+} is not due to a time-dependent process of relief from an intrinsically voltage-dependent block.

Mn^{2+}, Co^{2+}, and Cu^{2+} Decrease I_{Ba} Deactivation Speed

We further examined whether Mn^{2+}, Co^{2+}, and Cu^{2+}, besides decreasing I_{Ba} activation speed, also affect I_{Ba} deactivation kinetics upon repolarization. The voltage protocol routinely applied for this purpose is illustrated in Fig. 8*A*. Fifteen-ms test pulses delivered to elicit I_{Ba} were followed by step repolarizations at voltage levels variable from −20 to −60 mV (Fig. 8*A* only shows the return to −50 mV). In these experiments, the 2-s conditioning prepulse and the test pulse were set at −50 mV and −10 mV, respectively, so as to reduce the current size and thereby optimize the clamp control of tail currents. Fig. 8*B1*, *C1* and *D1* shows currents recorded in three different neurons in response to such voltage protocol, both in control conditions and in the presence of 150 μM Mn^{2+}, 300 μM Co^{2+}, or 3 μM Cu^{2+}. Currents are shown normalized to the peak amplitude of the tail currents resulting from step repolarization. It can be seen that tail-current decay was clearly slowed during the application of any of the three blocking ions. The decay phase of tail currents consistently followed a biexponential time course. The lumped deactivation time constant,

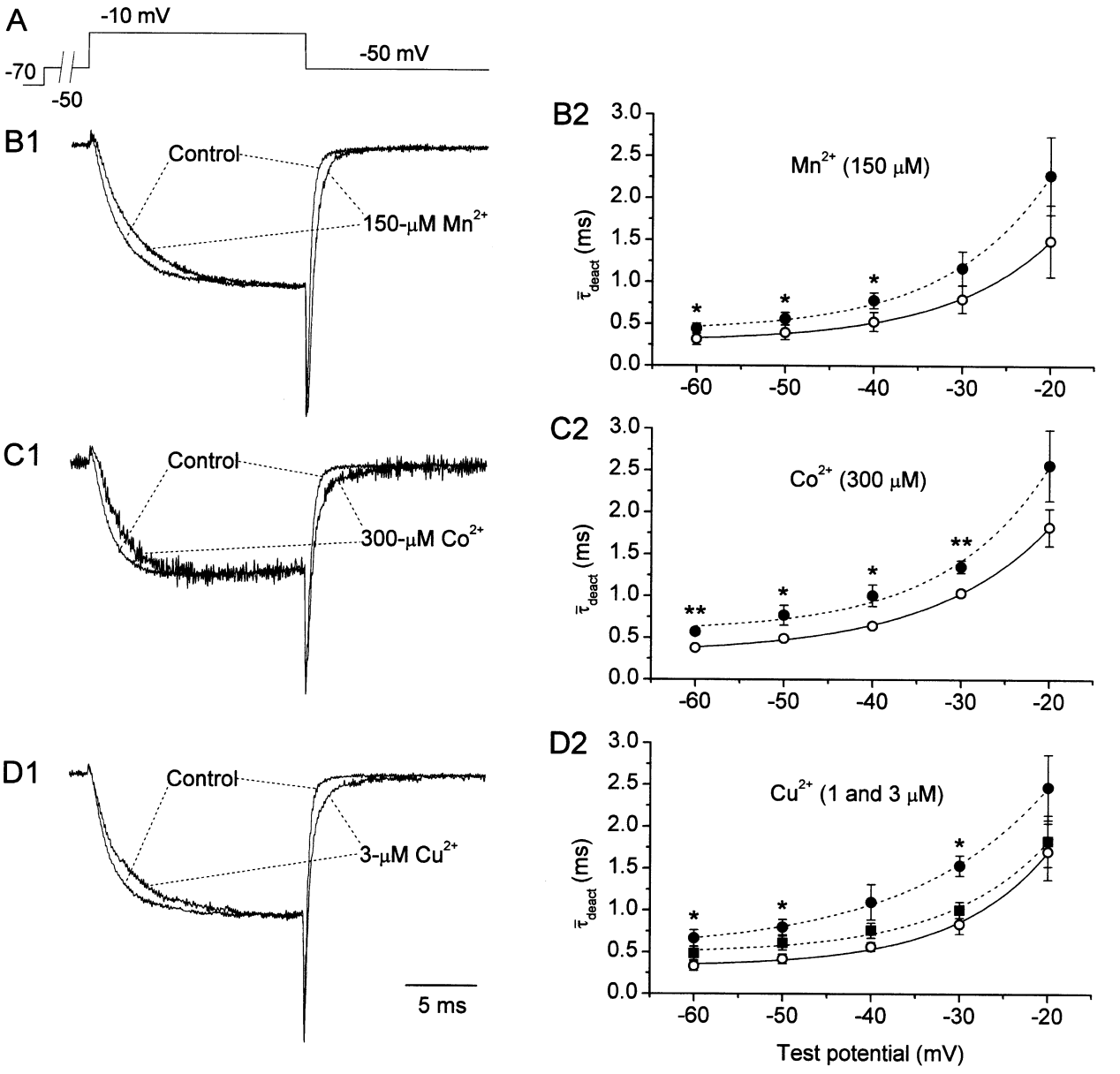

Fig. 8. Mn^{2+}, Co^{2+}, and Cu^{2+} slow repolarization-induced tail currents. *(A)* Voltage protocol applied to elicit tail currents: I_{Ba} was evoked with a fixed depolarizing step at −10 mV, followed by a repolarizing step at voltage levels variable from −20 to −60 mV (only the case of a repolarizing step at −50 mV is illustrated here). *(B–D)* Effects of 150 μM Mn^{2+} (*B*), 300 μM Co^{2+} (*C*), and 3 μM Cu^{2+} (*D*) on the kinetics of tail-current macroscopic deactivation. *Left panels*: I_{Ba} recorded in three representative neurons (cells B2617 in *B1*, B2N14 in *C1*, C2604 in *D1*) in response to the voltage protocol illustrated in panel *A*. Currents have been normalized to the peak amplitudes of tail currents elicited upon step repolarization. *Right panels:* average plots of the voltage dependence of the lumped deactivation time constant, $\bar{\tau}_{deact}$ (*empty circles*, *continuous lines*: control; *filled circles, dotted lines*: 150 μM Mn^{2+}, 300 μM Co^{2+}, or 3 μM Cu^{2+}; *filled squares* in *D2*: 1 μM Cu^{2+}). ***, $p < 0.001$; **, $p < 0.01$; *, $p < 0.05$ (*t*-test for paired data). Asterisks in panel *D2* refer to data on 3 μM Cu^{2+}; levels of significance for 1 μM Cu^{2+} were the same as for 3 μM Cu^{2+} at all test voltages. $n = 3$ (Mn^{2+}), 6 (Co^{2+}), and 4 (Cu^{2+}).

$\bar{\tau}_{deact}$ (calculated in the same way as the lumped activation time constant, $\bar{\tau}_{act}$; *see* above, Eq. 3) was consistently increased in the whole voltage range explored. At −30/−40 to −60 mV, percent $\bar{\tau}_{deact}$ increases were statistically significant and averaged ~40–50% for 150 μM Mn^{2+} (Fig. 8*B2*); ~30–60% for 300 μM Co^{2+} (Fig. 8*C2*); ~20–45% for 1 μM Cu^{2+}, and ~80–100% for 3 μM Cu^{2+} (Fig. 8*D2*).

Effects of Cu^{2+} on I_{Ba} Elicited by Action-Potential-Like Waveforms

The decrease in activation speed induced in residual currents by divalent metal cation blockers could be hypothesized to result in an extra reduction of I_{Ba} peak amplitude when these currents are elicited by short, phasic depolarizations, such as action

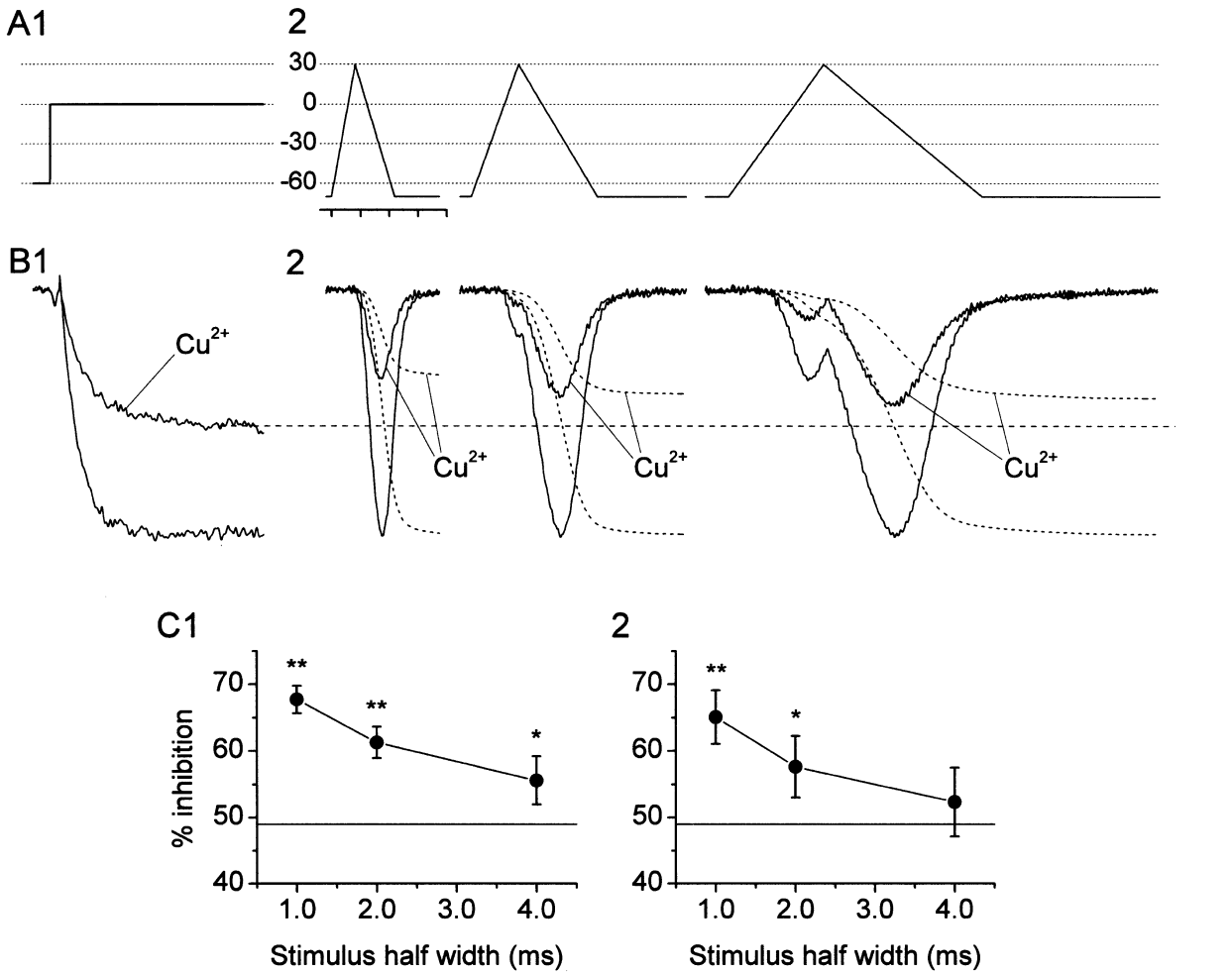

Fig. 9. Enhancement of Cu^{2+} inhibitory action in I_{Ba} elicited by short, action-potential-like phasic depolarizing stimuli. (*A*) Step (*A1*) and action-potential-like (*A2*) depolarizing test pulses delivered to evoke total I_{Ba}. The *y*-axis labels are mV, every *x*-axis division is 1 ms. Note the different half-widths of action-potential-like waveforms (APWs). (*B*) I_{Ba} recorded in a representative neuron (cell B3613) in response to the voltage-clamp protocols illustrated in panel *A*, both in control conditions and in the presence of 1 μM Cu^{2+} (all currents are Cd^{2+}-subtracted). In panel *B2*, the continuous lines are current traces, the dotted lines are the corresponding integrals over time (which represent the amount of charge transferred). Note that in both panel *B1* and *B2* currents and integrals were normalized to the peak values observed in control conditions. Actual control-current peak amplitudes were −658.1 pA (*B1*), −1018.6 pA (*B2, left*), −957.7 pA (*B2, middle*), −872.4 pA (*B2, right*); actual maximal values of control-current integrals were −988.3 fC (*B2, left*), −1739.3 fC (*B2, middle*), −3173.2 fC (*B2, right*). The horizontal, dashed line marks the relative level of I_{Ba}-amplitude inhibition observed in 1 μM Cu^{2+}, using the step protocol. (*C*) Average plots of Cu^{2+}-dependent percent inhibition of I_{Ba} peak amplitude (*C1*) and current integral (*C2*) as a function of the half width of APWs used as depolarizing stimuli ($n = 3$). The horizontal line in each sub-panel corresponds to the average level of Cu^{2+}-dependent percent inhibition of I_{Ba} amplitude as measured with step protocols (test potential = 0 mV). Statistical significance was calculated considering the percent inhibition measured with step protocols as the reference. **, $p < 0.01$; *, $p < 0.05$ (*t*-test for paired data).

potentials, instead of the step pulses employed experimentally (*see* also Magistretti et al., 2003). Again, this issue gets special importance in the case of Cu^{2+}, due to its possible physiological role(s) in neurotransmission and/or neuromodulation (*see* the Introduction). To test this possibility, we performed experiments in which I_{Ba} was evoked with action-potential-like waveforms (APWs) of variable duration (Fig. 9*A2*) in addition to the usual depolarizing step pulses (Fig. 9*A1*). The currents thus recorded in a representative neuron, both in the absence and in the presence of 1 μM Cu^{2+}, are shown in Fig. 9*B*. Step pulses returned a level of Cu^{2+}-dependent percent inhibition of ~49% (*horizontal, dashed line*). The peak amplitude of currents recorded in response to an APW of 100 mV in amplitude and 1 ms in half width (similar to the action potentials produced by PC superficial pyramidal neurons: *see* Tseng & Haberly, 1989) was decreased by Cu^{2+} to a higher degree (Fig. 9*B2*, *left panel*). When the APW half width was increased to 2 and 4 ms, the extra inhibition of current peak amplitude progressively decreased (Fig. 9*B2*, *middle* and *right panels*). Similar effects were also evident when the current integral, rather than peak

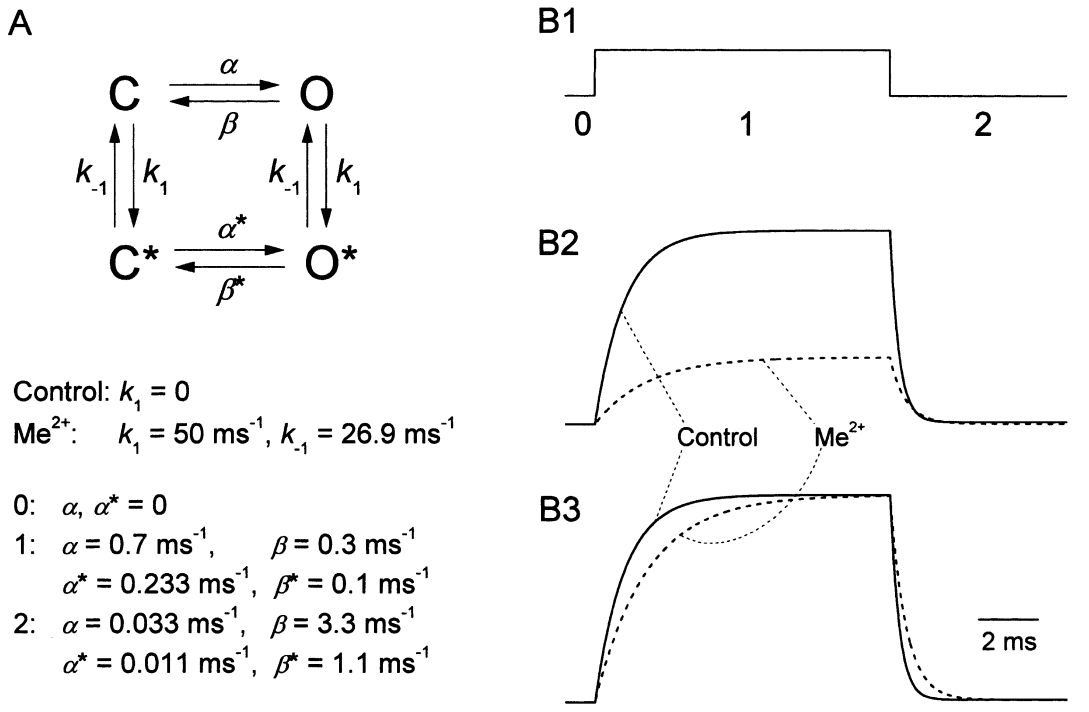

Fig. 10. Binding of a blocking cation to a single site of Ca^{2+} channels can result in both block and slowing of activation and deactivation kinetics of macroscopic currents if the rate constants of state transitions are affected by binding. (*A*) Elementary kinetic scheme of Ca^{2+}-channel opening-closing and binding-unbinding to a blocking cation. C and O are unbound closed and open states, C* and O* are closed and open states bound to the blocking cation. (*B*) Simulated activation-deactivation protocol (*B1*) and the time course of the probability of a channel to be in state O (open and unblocked) (*B2*, *B3*). The rate constants that govern the reactions schematized in the upper part of panel *A* have been assigned different, appropriate numerical values in the different epochs (0, 1, and 2) of the simulated protocol. These values are specified in the lower part of panel *A*. Note that the rate constants of the reactions between blocked states (α*, β*) are set at one third of those between unblocked states (α, β). Continuous and dotted lines in *B2* and *B3* were obtained, respectively, for concentrations of the blocking cation equal to zero ("Control": $k_1 = 0$) and to a value able to produce a ~65% block ("Me^{2+}": $k_1 = 50\ ms^{-1}$). In panel *B3* the traces have been normalized to their peak values to highlight the different time courses of the activation and deactivation phases.

amplitude, was considered, which is not surprising since 1 μM Cu^{2+} exerted a more prominent slowing effect on current activation than on current deactivation (*see* above). Average data for current peak amplitude and current integral are illustrated in Fig. 9*D*. The maximal degree of extra inhibition, observed with APWs of 1 ms in half width, was ~16–19%. In the case of APWs of 4 ms in half width, the differences in percent inhibition with respect to step-pulse protocols were small and, in the case of current integral, not statistically significant. These findings are consistent with an additional Cu^{2+}-dependent inhibitory action being exerted on I_{Ba} elicited by short, phasic depolarizations, as a consequence of the Cu^{2+}-induced reduction of I_{Ba} activation speed. As expected, the effects of this slowing of I_{Ba} activation kinetics appeared to be overcome as the duration of the stimulus applied was made progressively longer.

Discussion

The main results of the present study are: 1) Cu^{2+} is a very potent blocker of HVA Ca^{2+} channels in palaeocortical neurons, and 2) Mn^{2+}, Co^{2+}, and Cu^{2+} slow the activation kinetics of macroscopic HVA current with a mechanism different from a slow, depolarization-dependent relief from block.

Only a few studies so far have examined the effects of Cu^{2+} ions on neuronal voltage-dependent Ca^{2+} currents (Kasai & Neher, 1992; Nam & Hockberger, 1992; Horning & Trombley, 2001). We analyzed the effects of Cu^{2+} on HVA currents in rat PC neurons in the presence of 5 mM Ba^{2+} as the charge carrier, and found a very high blocking potency, with an IC_{50} of less than 1 μM and a Hill coefficient of about 1. This potency is much higher than those reported for Ca^{2+} currents expressed by neuroblastoma × glioma hybrid cells ($IC_{50} \approx 7$–14 μM; Kasai & Neher, 1992), rat olfactory bulb neurons ($IC_{50} \approx 30$ μM; Horning & Trombley, 2001), rat cerebellar Purkinje cells ($IC_{50} \approx 200$ μM; Nam & Hockberger, 1992), and chick dorsal-root-ganglion neurons ($IC_{50} \approx 800$ μM; Nam & Hockberger, 1992). It should be noted that the identity and concentration of the permeant ion can influence the apparent potency of blocker ions that act by competitively binding to a site located inside the permeation path:

for instance, this has been shown to be the case for the block exerted by Zn^{2+} on HVA Ca^{2+} channels in PC neurons (Magistretti et al., 2003). However, we also found that the percent block exerted by 1 μM Cu^{2+} on HVA currents recorded using Ca^{2+} at physiological concentration (1 mM) as the charge carrier was very similar to that observed using 5 mM Ba^{2+}. The finding that Cu^{2+} potently blocks voltage-gated Ca^{2+} channels in native brain neurons could have relevant implications in sight of the fact that Cu^{2+}, as well as Zn^{2+}, is likely to be present in the synaptic vesicles and terminals of several central synapses, and could be exocytotically released, thereby behaving as a physiological neuromodulator (Hartter & Barnea, 1988; Kardos et al., 1989; Sato et al., 1994; *see* also the Introduction). The possible importance of Zn^{2+}, the role of which as a physiological, synaptic neuromodulator is well established, and its release on the function of voltage-gated Ca^{2+} channels at central synapses has been discussed elsewhere (Magistretti et al., 2003).

We also found that all of the divalent metal cations here examined (Mn^{2+}, Co^{2+}, Cu^{2+}, and Cd^{2+}), besides exerting a blocking action on HVA channels, also significantly slow the activation kinetics of residual HVA currents. We could exclude that the latter effect is the consequence of a preferential inhibition of some fast-activating and -inactivating current component(s), since none of the components into which the I_{Ba} under study can be pharmacologically dissected displayed a fast-decaying early transient similar to that typically observed in metal cation-sensitive currents obtained by subtraction. The possibility that the slowing of I_{Ba} activation kinetics during Mn^{2+}, Co^{2+}, and Cu^{2+} block resulted from a voltage- and time-dependent relief from block upon depolarization could also be ruled out, since: 1) no voltage dependence of fractional block was found over the voltage range normally explored for eliciting I_{Ba} (−30 to +30 mV); and 2) no reduction of blocker-induced slowing of I_{Ba} was observed when depolarizing pulses were delivered from −30 mV (the threshold level for I_{Ba} detection) rather than −60 mV (the usual starting voltage level), thus excluding the existence of a saturating unblocking phenomenon of some current component over the same voltage span. Moreover, the finding that I_{Ba} deactivation is also markedly slowed during application of Mn^{2+}, Co^{2+}, and Cu^{2+} is further evidence that the changes of I_{Ba} kinetics induced by the three cations are not the consequence of an intrinsic voltage dependence of their blocking action. Indeed, if a process of slow relief from block was acting during depolarizing test pulses as a consequence of depolarization itself, one would expect that, upon repolarization, the tendency of the cation to re-block open channels would create an additional escape path from conducting to non-conducting states, thus accelerating, rather than slowing, the apparent deactivation kinetics (for details, *see* Magistretti et al., 2001). In this case, the blocking cation would produce, if anything, a decrease, and not an increase, of $\bar{\tau}_{deact}$ values derived from tail-current decay, which is in contrast with our data.

Other alternative mechanisms can be imagined to explain the observed effects of Mn^{2+}, Co^{2+}, and Cu^{2+} on Ca^{2+}-current activation kinetics, and in particular: i) binding of these metal cations to Ca^{2+} channels and the resulting block are state dependent, with closed states of Ca^{2+} channels being blocked with higher affinity than open states. In this case, activation (i.e., channel transition to open states) would lead to unbinding and, hence, to an unblocking process that, if slow enough, could result in apparent slowing of Ca^{2+}-current activation; ii) Mn^{2+}, Co^{2+}, and Cu^{2+} interfere with Ca^{2+}-channel gating kinetics. Although it does not appear possible to unequivocally discriminate between these two hypotheses on the sole basis of whole-cell data, our observation that I_{Ba} deactivation is also significantly slowed indicates that some effect must be exerted by the three metal cations on the speed of Ca^{2+} channel-state transitions, and points to hypothesis (ii) as a much more likely and parsimonious interpretation. Indeed, if Mn^{2+}, Co^{2+}, and Cu^{2+} slowed I_{Ba} activation with a state-dependent unblocking mechanism, channel deactivation upon repolarization would be either accelerated or basically unchanged, because in such a case the relative balance among blocked channels would be shifted towards closed states, which would provide an accelerated transition path from open to closed states. Only an intrinsic slowing of closed-to-open and open-to-closed state transitions can explain the concomitant occurrence of slower activation and deactivation in macroscopic currents.

Slowing effects on Ca^{2+}-channel activation/deactivation kinetics appear to be a common mechanism of action of many group VII*A*-II*B* metal cations. They have been reported for Ni^{2+} (McFarlane & Gilly, 1998; Magistretti et al., 2001), Zn^{2+} (Magistretti et al., 2003), Mn^{2+}, Co^{2+}, and Cu^{2+} (this paper), and Cd^{2+} (this paper; Taylor, 1988). In the case of Ni^{2+}, it has been previously suggested that such effects on Ca^{2+}-channel gating could be a specific feature of Ni^{2+} due to the geometric flexibility of this ion in aqueous solution, that can give rise to stable association with amino-acid residue, and/or the high degree of hydration of Ni^{2+} ions, that could allow them to promote weak interactions over large molecular distances (McFarlane & Gilly, 1998). Our data do not support this view, and show that different group VII*A*-II*B* metal cations exert similar effects on the gating properties of voltage-dependent Ca^{2+} channels, perhaps by acting on a common target site.

In the present study and a previous one (Magistretti et al., 2003) we have also shown that the slowing effect of Zn^{2+} and Cu^{2+} on Ca^{2+}-current activation kinetics can result in a significant, apparent potentiation of their channel-blocker action when the activation stimulus consists in a fast, phasic depolarization, such as the action potential. Again, this finding may be particularly interesting in sight of the known or presumed role of these metal cations as physiological modulators of neurotransmission. Indeed, it could be hypothesized that synaptically-released metal cations exert a feedback inhibition on presynaptic Ca^{2+} channels, thereby influencing neurotransmitter release: in such a case, even a moderate potentiation of Ca^{2+}-channel inhibition might result in a major effect on presynaptic function, since neurotransmitter release at central synapses is known to be strongly dependent (by the third to fourth power) on intracellular Ca^{2+} concentration (discussed in Magistretti et al., 2003).

Since the data reviewed above indicate that a number of group VII*A*-II*B* metal cations endowed with Ca^{2+}-channel blocker activity also affect Ca^{2+}-current kinetics, it could be hypothesized that the latter effect, although independent of channel-pore block per se (*see* above), is due to allosteric modifications of channel-gating mechanisms induced by the cations' binding to the same channel site, the occupancy of which results in channel block. This interpretation is not conflicting with the fact that only non-blocked channels can contribute to the currents, the activation and deactivation of which turns out to be slowed. Fig. 10 presents a simple kinetic model in which the binding of a blocker ion to a single Ca^{2+}-channel site is assumed to result not only in Ca^{2+}-channel block, but also in a decrease of closed-to-open and open-to-closed transition rates. If such decrease is big enough, and if the kinetic scheme is properly implemented, slowing of both current activation and deactivation can be produced by binding of the blocker ion (Fig. 10*B*). This model would provide a parsimonious, unitary explanation of the common ability of so many Ca^{2+}-channel blocking cations to interfere with Ca^{2+}-channel gating kinetics. However, it should be noted that, in the case of Ni^{2+}, other binding site(s), in addition to that accounting for channel block, have been proposed to exist and to be implicated in modifications of Ca^{2+}-channel gating. This was suggested by the existence of subtle differences in the concentration dependence of Ni^{2+}-dependent block and current slowing (Magistretti et al., 2001), and by a lack of correlation between the effects of Ni^{2+} on channel gating properties and its blocking action in different channel isoforms (Zamponi et al., 1996). The exact identification and localization of the binding site(s) implicated in metal-ion-dependent modifications of Ca^{2+}-channel gating will require further investigations.

References

Almers, W., Palade, P.T. 1981. Slow calcium and potassium currents across frog muscle membrane: measurements with a vaseline-gap technique. *J. Physiol.* **312:**159–176

Bean, B.P. 1989. Classes of calcium channels in vertebrate cells. *Annu. Rev. Physiol.* **51:**367–384

Carbone, E., Swandulla, D. 1989. Neuronal calcium channels: kinetics, blockade and modulation. *Prog. Biophys. Mol. Biol.* **54:**31–58

Chesnoy-Marchais, D. 1991. Kinetic properties and selectivity of calcium-permeable single channels in *Aplysia* neurones. *J. Physiol.* **367:**457–488

Chow, R.H. 1991. Cadmium block of squid calcium currents. Macroscopic data and a kinetic model. *J. Gen. Physiol.* **98**:751–770

Delahayes, J.F. 1975. Depolarization-induced movement of Mn^{2+} cations across the cell membrane in the guinea pig myocardium. *Circ. Res.* **36:**713–718

Doreulee, N., Yanovsky, Y., Haas, H.L. 1997. Suppression of long-term potentiation in hippocampal slices by copper. *Hippocampus* **7:**666–669

Fukuda, J., Kawa, K. 1977. Permeation of manganese, cadmium, zinc, and beryllium through calcium channels of an insect muscle membrane. *Science* **196:**309–311

Hagiwara, S., Byerly, L. 1981. Calcium channel. *Annu. Rev. Neurosci.* **4:**69–125

Hagiwara, S., Nakajima, S. 1966. Differences in Na and Ca spikes as examined by application of tetrodotoxin, procaine, and manganese ions. *J. Gen. Physiol.* **49:**793–806

Hagiwara, S., Takahashi, K. 1967. Surface density of calcium ions and calcium spikes in the barnacle muscle fiber membrane. *J. Gen. Physiol.* **50:**583–601

Hamill, O.P., Marty, A., Neher, E., Sakmann, B., Sigworth, F. 1981. Improved patch-clamp technique for high resolution current recordings from cells and cell free membrane patches. *Pfluegers* **391:**85–100

Hartter, D.E., Barnea, A. 1988. Evidence for release of copper in the brain: depolarization-induced release of newly taken-up ^{67}copper. *Synapse* **2:**412–415

Hille, B. 2001. Ion Channels of Excitable Membranes. Sinauer, Sunderland, MA

Holm, I.E., Andreasen, A., Danscher, G., Perez-Clausell, J., Nielsen, H. 1988. Quantification of vesicular zinc in the rat brain. *Histochemistry* **89:**289–293

Horning, M.S., Trombley, P.Q. 2001. Zinc and copper influence excitability of rat olfactory bulb neurons by multiple mechanisms. *J. Neurophysiol.* **86:**1652–1660

Huang, Y., Quayle, J.M., Worley, J.F., Standen, N.B., Nelson, M.T. 1989. External cadmium and internal calcium block of single calcium channels in smooth muscle cells from rabbit mesenteric artery. *Biophys. J.* **56:**1023–1028

Ibata, Y., Otsuka, N. 1969. Electron microscopic demonstration of zinc in the hippocampal formation using Timm's sulfide silver technique. *J. Histochem. Cytochem.* **17:**171–175

Kardos, J., Kovacs, I., Hajos, F., Kalman, M, Simonyi, M. 1989. Nerve endings from rat brain tissue release copper upon depolarization. A possible role in regulating neuronal excitability. *Neurosci. Lett.* **103:**139–144

Kasai, H., Neher, E. 1992. Dihydropyridine-sensitive and ω-conotoxin-sensitive calcium channels in a mammalian neuroblastoma-glioma cell line. *J. Physiol.* **448:**161–188

Kumamoto, E., Murata, Y. 1995. Characterization of GABA current in rat septal cholinergic neurons in culture and its modulation by metal cations. *J. Neurophysiol.* **74:**2012–2027

Lansman, J.B., Hess, P., Tsien, R.W. 1986. Blockade of current through single calcium channels by Cd^{2+}, Mg^{2+}, and Ca^{2+}.

Voltage and concentration dependence of calcium entry into the pore. *J. Gen. Physiol.* **88:**321–347

Ma, J.Y., Narahashi, T. 1993. Differential modulation of $GABA_A$ receptor-channel complex by polyvalent cations in rat dorsal root ganglion neurons. *Brain Res.* **607:**222–232

Magistretti, J., Brevi, S., de Curtis, M. 2001. Ni^{2+} slows the activation kinetics of high-voltage-activated Ca^{2+} currents in cortical neurons: evidence for a mechanism of action independent of channel-pore block. *J. Membrane Biol.* **179:**243–262

Magistretti, J., de Curtis, M. 1998. Low-voltage activated T-type calcium currents are differently expressed in superficial and deep layers of guinea-pig piriform cortex. *J. Neurophysiol* **79:**808–816

Magistretti, J., Castelli, L., Taglietti, V., Tanzi, F. 2003. Dual effect of Zn^{2+} on multiple types of voltage-dependent Ca^{2+} currents in rat palaeocortical neurons. *Neuroscience* **117:**249–264

McFarlane, M.B., Gilly, W.F. 1998. State-dependent nickel block of a high-voltage-activated neuronal calcium channel. *J. Neurophysiol.* **80:**1678–1685

Nam, S.C., Hockberger, P.E. 1992. Divalent ions released from stainless steel hypodermic needles reduce neuronal calcium currents. *Pfluegers Arch.* **420:**106–108

Narahashi, T., Ma, J.Y., Arakawa, O., Reuveny, E., Nakahiro, M. 1994. GABA receptor-channel complex as a target site of mercury, copper, zinc, and lanthanides. *Cell. Mol. Neurobiol.* **14:**599–621

Ochi, R. 1970. The slow inward current and the action of manganese ions in guinea-pig's myocardium. *Pfluegers* **316:**81–94

Ochi, R. 1975. Manganese action potentials in mammalian cardiac muscle. *Experientia* **31:**1048–1049

Perez-Clausell, J., Danscher, G. 1985. Intravesicular localization of zinc in rat telencephalic boutons. A histochemical study. *Brain Res.* **337:**91–98

Robbins, J., Trouslard, J., Marsh, S.J., Brown, D.A. 1992. Kinetic and pharmacological properties of the M-current in rodent neuroblastoma × glioma hybrid cells. *J. Physiol.* **451:**159–185

Sato, M., Ohtomo, K., Daimon, T., Sugiyama, T., Iijima, K. 1994. Localization of copper to afferent terminals in rat locus ceruleus, in contrast to mitochondrial copper in cerebellum. *J. Histochem Cytochem.* **42:**1585–1591

Schroder, H.D., Danscher, G., Jo, S.M., Su, H. 2000. Zinc-enriched boutons in rat spinal cord. *Brain Res.* **868:**119–122

Slomianka, L., Danscher, G., Frederickson, C.J. 1990. Labeling of the neurons of origin of zinc-containing pathways by intraperitoneal injections of sodium selenite. *Neuroscience* **38:**843–854

Swandulla, D., Armstrong, C.M. 1989. Calcium channel block by cadmium in chicken sensory neurons. *Proc. Natl. Acad. Sci. USA.* **86:**1736–1740

Taylor, W.R. 1988. Permeation of barium and cadmium through slowly inactivating calcium channels in cat sensory neurones. *J. Physiol.* **407:**433–452

Thèvenod, F., Jones, S.W. 1992. Cadmium block of calcium current in frog sympathetic neurons. *Biophys. J.* **63:**162–168

Trombley, P.Q., Shepherd, G.M. 1996. Differential modulation by zinc and copper of amino acid receptors from rat olfactory bulb neurons. *J. Neurophysiol.* **76:**2536–2546

Tseng, G-F., Haberly, L. 1989. Deep neurons in piriform cortex. II Membrane properties that underlie unusual synaptic responses. *J. Neurophysiol.* **62:**386–400

Vlachova, V., Zemkova, H., Vyklicky, L. 1996. Copper modulation of NMDA responses in mouse and rat cultured hippocampal neurons. *Eur. J. Neurosci.* **8:**2257–2264

Weiser, T., Wienrich, M. 1996. The effects of copper ions on glutamate receptors in cultured rat cortical neurons. *Brain Res.* **742:**211–218

Winegar, B.D., Kelly, R., Lansman, J.B. 1991. Block of current through single calcium channels by Fe, Co, and Ni. Location of the transition metal binding site in the pore. *J. Gen. Physiol.* **97:**351–367

Yang, J., Ellinor, P.T., Sather, W.A., Zhang, J.-F., Tsien, R.W. 1993. Molecular determinants of Ca^{2+} selectivity and ion permeation in L-type Ca^{2+} channels. *Nature* **366:**158–161

Zamponi, G.W., Bourinet, E., Snutch, T.P. 1996. Nickel block of a family of neuronal calcium channels: subtype- and subunit-dependent action at multiple sites. *J. Membrane Biol.* **151:**77–90